IBRO Neuroscience Reports 13 (2022) 356–363

Contents lists available at ScienceDirect

IBRO Neuroscience Reports

journal homepage: www.sciencedirect.com/journal/IBRO-Neuroscience-Reports

Research Paper

# Reducing Merkel cell activity in the whisker follicle disrupts cortical encoding of whisker movement amplitude and velocity

Clément E. Lemercier *, Patrik Krieger

*Faculty of Medicine, Institute of Physiology, Department of Systems Neuroscience, Ruhr University Bochum, Bochum, Germany*

ARTICLE INFO

*Keywords:*
Barrel cortex
Merkel cell
Neural coding
Somatosensation
Whisker follicle

ABSTRACT

Merkel cells (MCs) and associated primary sensory afferents of the whisker follicle-sinus complex, accurately code whisker self-movement, angle, and whisk phase during whisking. However, little is known about their roles played in cortical encoding of whisker movement. To this end, the spiking activity of primary somatosensory barrel cortex (wS1) neurons was measured in response to varying the whisker deflection amplitude and velocity in transgenic mice with previously established reduced mechanoelectrical coupling at MC-associated afferents. Under reduced MC activity, wS1 neurons exhibited increased sensitivity to whisker deflection. This appeared to arise from a lack of variation in response magnitude to varying the whisker deflection amplitude and velocity. This latter effect was further indicated by weaker variation in the temporal profile of the evoked spiking activity when either whisker deflection amplitude or velocity was varied. Nevertheless, under reduced MC activity, wS1 neurons retained the ability to differentiate stimulus features based on the timing of their first post-stimulus spike. Collectively, results from this study suggest that MCs contribute to cortical encoding of both whisker amplitude and velocity, predominantly by tuning wS1 response magnitude, and by patterning the evoked spiking activity, rather than by tuning wS1 response latency.

## 1. Introduction

Rodents actively use their whiskers to explore their environment, discriminate between objects and interact socially with conspecifics. The angle, speed and bending features of the whiskers, enable inferring of information about the physical characteristics of objects being explored (Diamond et al., 2008). To detect and perceive a large variety of tactile features, distinct classes of low threshold mechanosensory receptors (LTMRs), innervating the whisker follicle-sinus complex (FSC) (Ebara et al., 2002; Fundin et al., 1994; Rice et al., 1986, 1997; Tonomura et al., 2015), translate the mechanical forces of whisker movement into trains of action potentials along primary trigeminal afferent neurons (Abraira and Ginty, 2013, Furuta et al., 2020; Gottschaldt et al., 1973; Severson et al., 2017). The neural code of whisker movement from neurons of the trigeminal ganglion (Ahissar et al., 2000; Bale et al., 2015; Jones et al., 2004; Szwed et al., 2003) then travels sequentially in a somatotopic manner through the brainstem trigeminal nuclei and somatosensory thalamic nuclei to the primary somatosensory barrel cortex (wS1) where information is integrated (Adibi, 2019; Ahissar et al., 2000, 2001; Bosman et al., 2011; Krieger and Groh, 2015; Petersen, 2007; Sakurai et al., 2013). While knowledge about sensory processing along the trigemino-thalamo-cortical pathways is progressing, the precise functions played by the different whisker mechanoreceptor subtypes in cortical encoding of whisker movement features are currently not fully understood.

Whisker mechanoreceptors have been classified according to their morphological features into: Merkel, lanceolate, club-like, Ruffini endings (Ebara et al., 2002; Furuta et al., 2020; Rice et al., 1986, 1997; Tonomura et al., 2015) and, as well as slowly or rapidly adapting encoders (SA and RA), according to their rates of adaptation to sustained mechanical stimulus (Gottschaldt et al., 1973). Their morphological, positional, and discharge features are factors determining their properties in encoding diverse features of whisker movement (Furuta et al., 2020; Gottschaldt et al., 1973). Among the most prominent whisker mechanoreceptors is the Merkel cell-neurite complex (Gottschaldt and Vahle-Hinz, 1981; Halata et al., 2003; Iggo and Muir, 1969; Woo et al.,

*Abbreviations:* CDF, cumulative distribution function; FSC, follicle-sinus complex; IQR, interquartile range; K14, keratin 14; LTMR, low threshold mechanoreceptor; MC, Merkel cell; PSTH, peristimulus time histograms; PW, principal whisker; RA, rapidly adapting; SA, slowly adapting; TeNT, tetanus neurotoxin light-chain subunit; wS1, primary somatosensory barrel cortex.

* Correspondence to: Departement of Systems Neuroscience, Ruhr University Bochum, Universitätsstraße 150, D-44780 Bochum, Germany.
*E-mail address:* clement.lemercier@rub.de (C.E. Lemercier).

https://doi.org/10.1016/j.ibneur.2022.09.008
Received 8 July 2022; Accepted 26 September 2022
Available online 29 September 2022

2015) in which mechanically excitable cells (i.e. Merkel cells, MCs) synaptically excite primary trigeminal afferent neurons to fire SA impulses (Chang et al., 2016; Higashikawa et al., 2019; Hoffman et al., 2018; Ikeda et al., 2014; 1994; Maksimovic et al., 2014; Maricich et al., 2009; Nakatani et al., 2015; Woo et al., 2014; 2015). The activity of MCs strongly correlates with whisker displacement amplitude (Ikeda et al., 2014), and MC-associated afferents show robust coding of whisker self-movement, angle, and whisk-phase during whisking (Furuta et al., 2020; Severson et al., 2017). Considering that MCs constitute the primary sites for translation of whisker movement at SA afferents, and that associated first-order trigeminal ganglion SA neurons encode whisker movement amplitude and velocity respectively by their response magnitude and latency (Kwegyir-Afful et al., 2008; Lottem et al., 2015; Shoykhet and Daniel, 2000; Stüttgen et al., 2008), a reduction in MC activity is hypothesized to affect cortical encoding of these two modalities.

To assess this possibility, wS1 neurons were recorded juxtacellularly in anesthetized transgenic mice with established reduced mechanoelectrical coupling at MC-associated SA primary sensory afferents (Hoffman et al., 2018). Whiskers were deflected with six different deflection paradigms involving 3 different plateau amplitudes and 3 different ramp velocities and the coding properties of wS1 neurons were analysed and compared to littermate control mice. Data from the present study indicate that a reduction in MC activity increases wS1 sensitivity to whisker deflection. In condition of reduced MC activity, wS1 neurons response magnitude univariately coded the variation in whisker deflection amplitude or velocity. Nevertheless, wS1 neurons retained the ability to differentiate stimulus features based on the timing of their response. Collectively, our results suggest that MCs exert a predominant role in tuning the cortical response magnitude rather than in tuning the cortical response latency.

## 2. Materials and methods

### 2.1. Animals

Transgenic mice expressing tetanus neurotoxin light-chain subunit (TeNT) in MCs were obtained by crossing hemizygous $K14^{Cre}$ male with homozygous $Rosa26^{floxstopTeNT\text{-}GFP}$ female mice as described in Hoffman et al. (2018). Genotyping was performed at the Department of Physiology & Cellular Biophysics, Columbia University, New York, USA. Experiments involved 6 adult mice of both sexes comprising three littermate controls ($Rosa26^{floxstopTeNT\text{-}GFP}$) and three mice expressing TeNT in MCs ($K14^{Cre};R26^{TeNT}$). Animal experimentation was conducted according to both European Union and German animal welfare regulations and was approved by the local government ethics committee (Landesamt für Natur, Umwelt und Verbraucherschutz, Nordrhein-Westfalen, Germany).

### 2.2. Surgery and recording

Mice were anesthetized by an intraperitoneal injection of a saline mixture of urethane (1.2–1.4 g/kg, Sigma-Aldrich Chemie Gmbh, Steinheim, Germany) and acepromazine (0.5 mg/kg). Body temperature was monitored and maintained at 37 °C using a closed-loop heating pad (FHC Inc., Bowdoin, ME, USA). Oxygen was supplied continuously, and the breathing rate was monitored on an oscilloscope with a piezoelectric disc (27 mm diameter) placed beneath the animal's torso (Zehendner et al., 2013). When necessary, anesthesia was maintained with a supplementary injection of urethane (0.1–0.15 g/kg). The scalp was locally anesthetized with bupivacaine (0.25 %) and incised. A head plate was fixed to the cranium with dental acrylic, the animal's head was stabilized, and a craniotomy of ~1 $mm^2$ was made over the left wS1 cortex at 1.8 mm posterior to the bregma and 3 mm lateral to the midline. The bath solution that was placed on top of the craniotomy comprised sterile physiological saline (0.9 % NaCl). Juxtacellular recordings from wS1 neurons of head-fixed mice were made with 4–6 MΩ patch pipettes made from borosilicate filament glass (Hilgenberg GmbH, Malsfeld, Germany; outer diameter: 1.5 mm, inner diameter: 0.86 mm) with a Sutter P-1000 puller (Sutter Instruments, Novato, CA, United States) filled with an extracellular solution containing 135 NaCl, 5.4 KCl, 1.8 $CaCl_2$, 1 $MgCl_2$, 5 HEPES (mM, pH ~7.2). Positioning of the recording electrode was controlled by a motorized micromanipulator (SM-1; Luigs & Neumann GmbH, Ratingen, Germany). Signals were amplified (Axo-Clamp 2B amplifier; Axon Instruments/Molecular Devices, LLC. San Jose, CA, USA), high-pass filtered at 300 Hz and sampled at 20 kHz (Digidata 1320 A; Axon Instruments) and visualized using pClamp 8 software (Axon Instruments).

### 2.3. Whisker deflection paradigms

Whiskers were all trimmed to the same length of ~1 cm to ensure equal movement when deflected. Once a neuron was approached, a thin wooden stick (diameter: 2 mm) was used as a probe to deflect the whiskers manually and individually, and an audio monitor was used to identify the whisker that evokes the strongest response with shortest latency (i.e. the principal whisker, PW). The PWs were deflected using a ramp-and-hold movement by inserting their tips into a glass capillary (placed ~1 mm from the muzzle) glued to a piezo wafer (PL127.10; PI Ceramics GmbH, Lederhose, Germany) controlled by a piezo filter and amplifier (Sigmann Elektronik GmbH, Hüffenhardt, Germany). The plateau amplitude (i.e. total displacement) of the piezo wafer was monitored with a video camera (USB8MP02G-SFV; Ailipu Technology Co., Ltd., Shenzhen, China) and peak ramp velocity was estimated as the ratio between piezo plateau amplitude to piezo-amplifier transition time. The maximal peak ramp velocity was thus estimated to be ~0.6 mm/ms to the maximal plateau amplitude achievable of ~1.2 mm, which considers displacement due to ringing. Spiking activity of wS1 neurons was measured across six distinct whisker deflection paradigms, including three paradigms with varying plateau amplitude at constant ramp velocity (displacement of ~1.2, ~0.5 and ~0.25 mm at a velocity of ~0.6 mm/ms) and three paradigms with varying ramp velocity at constant plateau amplitude (velocity of ~0.6, ~0.12 and ~0.06 mm/ms at a displacement of ~1.2 mm). The holding time of the piezo wafer was set at 100 ms. Deflection paradigms were presented as a random sequence of recording blocks comprising 20 stimuli delivered at 0.5 Hz. For each deflection paradigm, spiking activity was monitored over 3 recording blocks (i.e. 60 deflections per deflection paradigm). An additional paradigm was designed to evaluate change in the response adaptation to repetitive whisker deflection and comprised trains of 8 deflections at 8 Hz (displacement of ~1.2 mm at a velocity of ~0.6 mm/ms, piezo wafer holding time set at 25 ms) delivered at 0.2 Hz over 3 recording blocks of 20 sweeps.

### 2.4. Histology

At the end of the experiment, animals were overdosed with urethane (3 g/kg), transcardially perfused with paraformaldehyde 4 % (V/V in phosphate buffer) and their brains were removed and prepared for flattened corticotangential sectioning, as described by Lauer et al., (2018). Cortical sections were stained for cytochrome oxidase, and layer IV barrel-field cytoarchitecture was visualized under bright-field light microscopy. Mystacial pads were dissected, cryoprotected in a 0.1 M phosphate buffer solution containing 30% sucrose (w/v) and cut into 50 μm thick transversal sections with a cryostat microtome (CM3050S; Leica Biosystems, Wetzlar, Germany). Sections were counterstained with the nuclear dye 4′,6-Diamidine-2′-phenylindole dihydrochloride (DAPI; Sigma-Aldrich, Germany) and actin filaments were labeled with the fluorescent conjugate ATTO 647-phalloidin (Hypermol EK, Bielefeld, Germany). Optical sections of the whisker follicle-sinus complex were acquired by confocal-like optical sectioning with an Apotome Microscope (Axioimager Z1; Carl Zeiss Microscopy GmbH, Jena,

Germany). The expression of TeNT-GFP in *Cre*-positive mice was confirmed by the presence of a green fluorescence signal in the MC-dense region of the whisker FSC.

### 2.5. Data analysis

Spike detection was done with the template search function of the software pClamp 11.2 (Axon Instruments), and spontaneous spiking and peri-stimulus spike timestamps were determined. For each recorded neuron, spontaneous spiking activity was estimated over segments of 1 s distantly located from the deflection onset (1 s). To assess the overall effect of reducing MC activity on cortical spiking activity, the number of evoked spikes, response probability (whether spikes were elicited or not) and first-spike latency to whisker protraction were first measured over a 100 ms response window. Response adaptation to repetitive whisker deflection (including responses to protraction and retraction) was evaluated by quantifying and comparing the number of evoked spikes at each deflection over a 100 ms response window. Changes in response magnitude (i.e. evoked spike count) to varying whisker protraction amplitude or velocity were quantified over a shorter response window of 30 ms. Peristimulus time histograms (PSTH) were determined over a window of 150 ms (10 ms bin size) including 50 ms prior to, and 100 ms after, stimulus onset. Cumulative distribution functions (CDFs) derived from PSTHs were used to analyze the temporal aggregation of the evoked spiking activity. Differences between CDFs in response to varying whisker deflection intensity (either amplitude or velocity) were evaluated by plotting CDFs at intermediary ($y$) or minimal ($y'$) deflection intensity against CDFs at maximal ($x$) deflection intensity (i.e. $y = f(x)$) and differences were quantified in a pooled manner (across $y$ and $y'$) with the following equation:

$$\Delta CDF = \frac{\sum_{i=1}^{n}(y_i - x_i) + (y'_i - x_i)}{2} \quad (1)$$

### 2.6. Statistics

Statistical analysis was performed using the R software (R Core Team, 2021) and the 'PMCMRplus' package (Pohlert, 2020). To report statistics in text, controls and mice expressing TeNT in MCs are respectively abbreviated as 'CON' and '$MC_{TeNT}$'. Differences between and within experimental groups were respectively evaluated with a Wilcoxon rank sum test and with a Friedman test. A $p$-value $< 0.05$ was considered statistically significant. Unless specified, data are reported in the text as Median and Interquartile ranges (IQR, i.e. the differences between Q3 and Q1). Sample size ($n$) is reported in the figure legends. Figures were produced with the R package 'ggplot2' (Wickham, 2016).

## 3. Results

### 3.1. Expression of TeNT in the MC-dense region of the whisker FSC and barrel-field cytoarchitecture

To reduce mechanoelectrical coupling at Merkel endings, the vesicular release machinery of MCs was blocked by expressing TeNT in cells expressing the K14 epidermal marker (Hoffman et al., 2018; Morrison et al., 2009; Van Keymeulen et al., 2009; Woo et al., 2010; Yamamoto et al., 2003). Genetic expression of TeNT-GFP in the whisker FSC was confirmed by a green fluorescence signal located in the MC-dense region (MDR) at the level of the ring sinus (RS) between the ringwulst (RW) and the inner canonical body (ICB) (Ebara et al., 2002; Rice et al., 1986; Whiteley et al., 2015) (Fig. 1A-1B). The effect of reducing MC activity on layer IV wS1 cytoarchitecture was evaluated on flattened cortico-tangential sections stained for cytochrome oxidase (Land and Simons, 1985; Lauer et al., 2018; Welker and Woolsey, 1974) (Fig. 1C-1D). A reduction in MC activity was not associated with a noticeable change in individual barrel sizes from respectively identified barrel rows (observation from one slice of both groups).

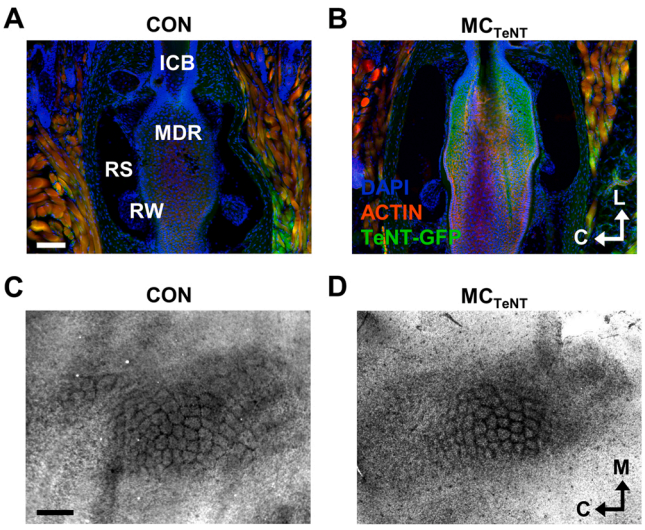


**Fig. 1. Expression of TeNT in the MC-dense region of the whisker FSC and barrel-field cytoarchitecture. (A-B)** Longitudinal sections of the whisker FSC stained for cell nuclei and actin filaments from control (A) and $MC_{TeNT}$ (B) mice. Note the presence of a green fluorescence signal indicative of the expression of TeNT-GFP at the level of the MC-dense region (MDR) of the whisker FSC in $MC_{TeNT}$ mice. ICB: Inner canonical body; MDR: Merkel cell dense region; RS: Ring sinus; RW: Ringwulst. Scale bar, 100 μm. C, caudal; L, lateral. **(C-D)** Flattened tangential sections of layer IV wS1 cortex (left hemisphere) stained for cytochrome oxidase from control (C) and $MC_{TeNT}$ mice (D). Scale bar, 500 μm. C, caudal; L, lateral.

### 3.2. Reducing MC activity increases wS1 sensitivity to whisker deflection

The median depth, relative to the pia mater, of the recorded wS1 neurons was similar between the two experimental groups (CON = 494 μm (230), n = 9; $MC_{TeNT}$ = 605 μm (177), n = 10; $p = 0.4967$ - Fig. 2A). The effect of reducing MC activity on whisker-evoked wS1 spiking activity was first evaluated by pooling the data collected across the six different whisker deflection paradigms with varying amplitude or velocity.

Although expression of TeNT in MCs has previously been reported to reduce mechanoelectrical coupling at SA afferents by about ~50 % (Hoffman et al., 2018) our data indicate that reducing MC activity increased wS1 neurons' sensitivity to whisker deflection (Fig. 2B-2C). This effect manifested in an increase in the number of whisker-evoked spikes (CON = 1.17 spikes (1.63); $MC_{TeNT}$ = 2.72 spikes (1.30), $p = 0.0349$ - Fig. 2B) and in response probability (CON = 0.72 (0.40); $MC_{TeNT}$ = 0.93 (0.18), $p = 0.0279$ - Fig. 2C), but occurred without significant change in first-spike latency (CON = 15.74 ms (3.73); $MC_{TeNT}$ = 10.66 ms (6.61), $p = 0.1333$ - Fig. 2D) nor in spontaneous spiking activity (CON = 2.17 Hz (5.14); $MC_{TeNT}$ = 4.65 (4.83), $p = 0.2775$ - data not shown).

The increased sensitivity to whisker deflection was accompanied by a lack of response adaptation to repetitive whisker deflection. Indeed, response adaptation was significantly observed in controls between the 1st/7th, and 1st/8th deflection pairs (1st = 1.78 spikes (0.34), 7th= 0.98 (0.26), 8th = 0.94 (0.26), data expressed as Mean (SEM); 1st/7th: $p = 0.0300$; 1st/8th: $p = 0.0214$ - Fig. 2E) but not under conditions of reduced MC activity (1st = 2.83 spikes (0.57), 7th = 2.11 (0.75), 8th = 1.95 (0.78), data expressed as Mean (SEM); 1st/7th: $p = 0.3574$; 1st/8th: $p = 0.6384$ - Fig. 2E), although spiking activity tended on average to decrease.

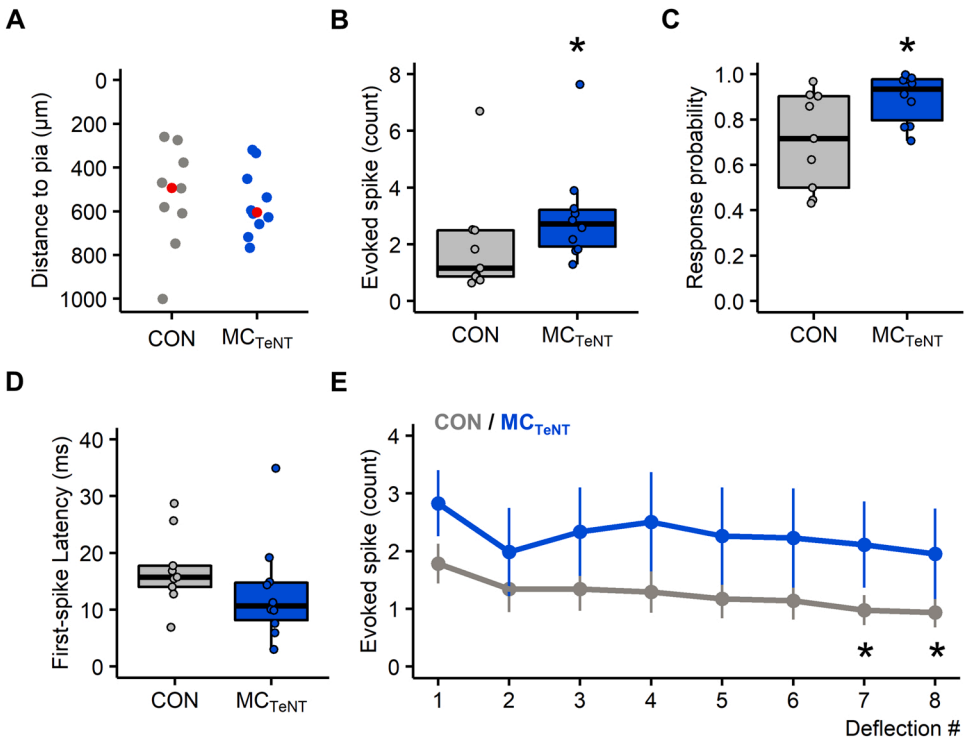


**Fig. 2. Overall effect of reducing MC activity on whisker-evoked wS1 spiking, response probability, first-spike latency, and response adaptation to repetitive deflection.** **(A)** Relative depth distribution to pia of the recorded wS1 neurons (CON: n = 9; $MC_{TeNT}$: n = 10), red markers indicating the median recording depth. **(B-D)** Boxplots showing the grand-average effect (collapsed across the six different whisker deflection paradigms) of reducing MC activity on the number of whisker-evoked spikes, response probability and first-spike latency (over a 100 ms response window) (CON: n = 9; $MC_{TeNT}$: n = 10). **(E)** Average number of evoked spikes along 8 repetitive whisker deflection delivered at 8 Hz (CON: n = 7; $MC_{TeNT}$: n = 7), data shown as Mean ± SEM. (*) Indicates significant differences in controls between 1st/7th and 1st/8th deflection pairs. (A-D) Wilcoxon rank sum test. (E) Friedman test followed by Conover's all-pairs posthoc test.

### *3.3. Reducing MC activity alters the response magnitude of wS1 neurons to varying whisker deflection amplitude and velocity*

During ramp-and-hold whisker deflection, wS1 neurons exhibit response magnitude and timing that generally depend on whisker deflection amplitude and velocity (Ito, 1985; Ito and Kato, 2002; Pinto et al., 2000; Wilent and Contreras, 2004), with strong and weak deflection amplitude or velocity leading respectively to strong/short and weak/long response magnitude and latency. Decreasing whisker deflection amplitude or velocity decreased the evoked spiking activity in controls but not in conditions of reduced MC activity (varying amplitude: CON, $p = 0.0030$; $MC_{TeNT}$, $p = 0.1496$; varying velocity: CON, $p = 0.0207$; $MC_{TeNT}$, $p = 0.2765$) – (Fig. 3A-3B and Table S1). Under reduced MC activity, the coding properties of wS1 were partially preserved, as seen in the decreased response probability when deflection amplitude was reduced (CON, $p = 0.0017$; $MC_{TeNT}$, $p = 0.0122$) – (Table S1) and with increased first-spike latency when deflection amplitude or velocity was reduced (varying amplitude: CON, $p = 0.0043$; $MC_{TeNT}$, $p = 0.002$; varying velocity: CON, $p < 0.001$; $MC_{TeNT}$, $p = 0.0025$) – (Table S1). Nevertheless, response probability and first-spike latency at low deflection amplitude or low velocity were on average higher and faster than in controls (Table S1). Taken together, these data suggest that MCs contribute to cortical encoding of both whisker movement amplitude and velocity, predominantly by tuning wS1 response magnitude rather than by tuning its firing latency and probability.

In controls, inspection of PSTHs indicates that variations in whisker deflection amplitude or velocity influence the patterning of the evoked spiking activity. Effects varied from patterns with rather fixed timing over a short period at strong deflection intensities, through patterns with more variable timing over a longer period at weaker deflection intensities (Fig. 3C-3D). Interestingly, PSTHs under reduced MC activity, especially for varying deflection velocity, appear to exhibit less change in the temporal aggregation of the evoked spiking activity than in controls (Fig. 3C-3D). To evaluate changes in whisker-evoked spike patterns, cumulative distribution functions (CDFs) were derived from PSTHs, and changes in CDFs at intermediary and minimal deflection intensity (either amplitude or velocity) were assessed against CDFs at maximal deflection intensity used as a reference (Fig. 4, see materials and methods).

In controls, CDF rates of evoked spiking activity decreased, as deflection amplitude or velocity decreased (Fig. 4A and 4D), indicating that lowering whisker deflection intensity causes spiking activity to aggregate less suddenly and more distributed over time. Shifts in CDF rates across whisker deflection intensities were on average weaker in condition of reduced MC activity (Figs. 4B and 4E) indicating that spiking activity tended to aggregate equally in time, independently of changes in whisker deflection amplitude or velocity. In respect to control, differences in CDFs for varying whisker deflection amplitude or velocity were weaker under reduced MC activity (varying amplitude: $p = 0.0563$ - Fig. 4C; varying velocity: $p = 0.0360$ - Fig. 4F). Taken together, these data suggest that, beyond contributing to wS1 response magnitude, MCs also contribute to the patterning of wS1 spiking activity.

## 4. Discussion

Data from this study suggest that reducing MC activity increases wS1 neuron sensitivity and response probability to whisker deflection. As activity of MCs and associated afferents strongly correlate with whisker movement during passive and active touch (Furuta et al., 2020; Hoffman et al., 2018; Ikeda et al., 2014; Severson et al., 2017), a reduction in their activity was presumed to produce the opposite effect on wS1 activity. Nevertheless, increased cortical sensitivity to cutaneous touch of glabrous skin has been recently reported in the somatosensory cortex (S1) in response to genetic ablation of MCs (Emanuel et al., 2021). The interpretation for the shift in S1 sensitivity was that MC-associated afferents recruit subcortical elements involved in setting S1 sensitivity. Another interpretation, albeit complementary but more speculative, comprises a role of MC-associated afferents in gating early sensory inputs from other LTMRs by interacting potentially with the inhibitory circuitry of the trigeminal ganglion (Hayasaki et al. 2006). However, putative compensatory mechanisms from other whisker LTMRs occurring in response to reduced mechanoelectrical coupling at

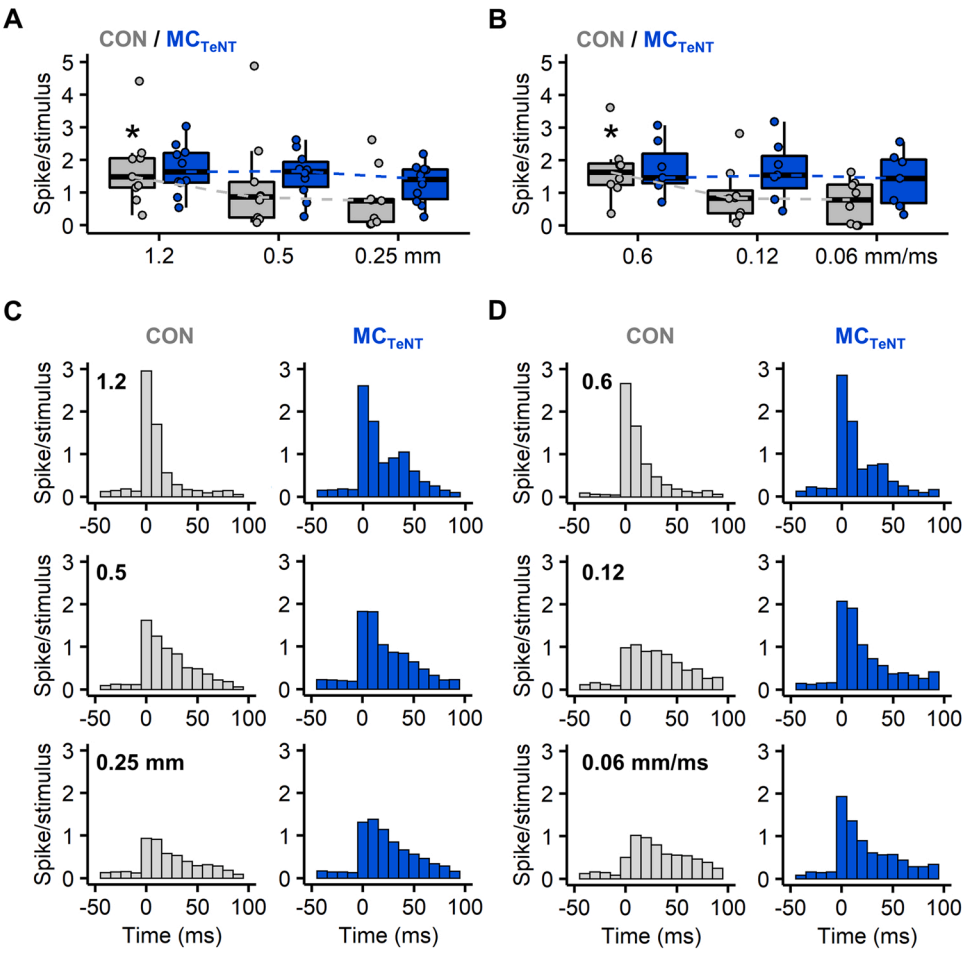


**Fig. 3. Effect of reducing MC activity on whisker-evoked wS1 spiking activity in response to varying whisker deflection amplitude or velocity. (A-B)** Average number of evoked spikes (over a 30 ms response window) across the different whisker deflection paradigms with varying deflection amplitudes (A) or velocities (B). Data from MC$_{TeNT}$ mice are displayed in blue. (*) Indicates that spiking activity in controls significantly decreases when deflection amplitude or velocity is varied (Friedman test). Dashed lines link medians. **(C-D)** Population PSTHs (average response over 60 sweeps, bin width 10 ms) for each deflection paradigm with varying amplitude (C) or velocity (D). (A-D) Varying amplitude: CON, n = 9; MC$_{TeNT}$, n = 10 - Varying velocity: CON, n = 8; MC$_{TeNT}$, n = 7.

MC-associated afferents have also to be considered.

In the sample of recorded neurons, increased sensitivity to whisker deflection was suggested to occur with a lack of response adaptation to repetitive deflection. Although spiking activity to repetitive deflection decreased, on average, in conditions of reduced MC activity, this effect did not reach statistical significance. Low sample size and higher spiking variability under conditions of reduced MC activity are most likely to be the cause. While neural adaptation along the whisker-barrel pathway occurs at all stages of sensory processing (Adibi and Lampl, 2021), primary sensory neurons of the trigeminal ganglion exhibit little adaptation to repeated whisker deflection, in contrast to subsequent sensory relays (Adibi and Lampl, 2021; Ganmor et al., 2010). Adaptation appears to be rather inherited in subsequent sensory relays, making the absence of sensory adaptation taking place at the level of the cortex difficult to interpret under conditions of reduced MC activity. Additional experiments will allow to better test this observation.

The data of the present study suggest that MCs contribute to cortical encoding of both whisker deflection amplitude and velocity, predominantly by tuning the cortical response magnitude and by patterning the evoked spiking activity. Nevertheless, under conditions of reduced MC activity, cortical encoding of whisker deflection amplitude and velocity was still preserved, notably in terms of changes in first-spike latency and response probability. Cortical first-spike latency thus may rely on other RA whisker LTMR subtypes, such as lanceolate- and club-like endings. Indeed, these two LTMR subtypes exhibit faster response latency than SA Merkel endings (Furuta et al., 2020). Nevertheless, it has been recently reported that, depending on their location in the whisker FSC (i.e. deep vs. superficial), Merkel endings exhibit different adapting properties (i.e. SA vs. RA) and therefore differential sensitivities to whisker movement (Furuta et al., 2020). Therefore, in the present study, the reported cortical effects are assumed to arise from a reduction in mechanoelectrical coupling at both types of Merkel endings.

Whisker movement amplitude and velocity are features used by rodents for inferring information about their environment (Arabzadeh et al., 2005; Pammer et al., 2013). Along the whisker-barrel pathway, whisker movement amplitude and velocity are respectively better represented by response magnitude and timing (Bale et al., 2015; Kwegyir-Afful et al., 2008; Lottem et al., 2015; Shoykhet and Daniel, 2000) although wS1 neurons are more sensitive to whisker movement velocity than to amplitude (Pinto et al., 2000). Analysis of coding strategies of whisker movement along the whisker-barrel pathway indicated that the majority of the information about the stimulus identity is retained in the timing of the first post-stimulus spike (Bale and Petersen, 2009; Bale et al., 2015; Panzeri et al., 2001; Petersen et al., 2001). Therefore, as previously reported with genetic ablation of MCs (Maricich et al., 2012), our data seem to suggest that mice with reduced MC activity can still rely on their whiskers through other LTMR subtypes to perform tactile behaviors such as texture discrimination tasks. In addition to being the main organ for tactile perception in mice, whiskers self-motion combined with those of facial hairs has been proposed to contribute to facial proprioception in mice (Severson et al., 2017, 2019). Considering the ability of MC-associated afferents to signal both static and dynamic whisker self-movement in their rates of sustained discharge, this LTMR might constitute a good candidate in contributing to facial proprioception in mice.

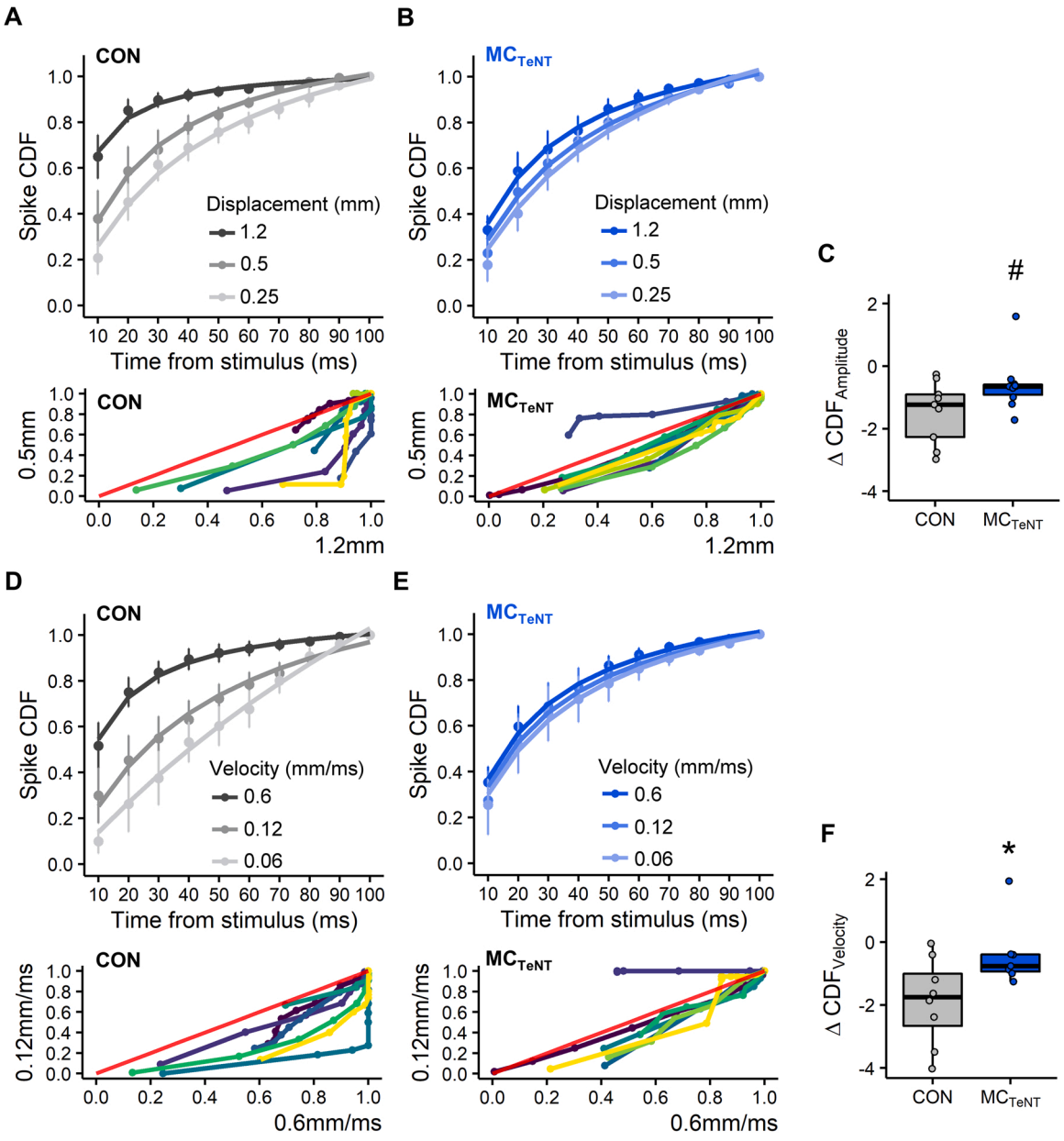


**Fig. 4. Effect of reducing MC activity on the temporal profile of whisker-evoked wS1 spiking activity in response to varying whisker deflection amplitude or velocity. (A-B)** Change in spike CDFs in response to varying whisker deflection amplitude from control (A) and $MC_{TeNT}$ mice (B). Below is shown the crossed-CDF variation between maximal and intermediary deflection amplitude for each individual neuron; red line denotes an identical distribution (i.e. $f(y) = f(x)$). **(C)** Pooled variation in CDFs across maximal/intermediary and maximal/minimal whisker deflection amplitude, # is indicative of $p = 0.0563$. **(D-F)** Identical panel structure to (A-C) for data obtained with varying whisker deflection velocity. (A-B and D-E) data shown as Mean ± SEM. Fits computed with non-linear least squares regression, Pearson's Goodness-of-Fit: $p < 0.05$. (C and F) Wilcoxon rank sum test. (A-F) Varying amplitude: CON, n = 9; $MC_{TeNT}$, n = 10 - Varying velocity: CON, n = 8; $MC_{TeNT}$, n = 7.

## 5. Conclusion

The major outcome of this preliminary study indicates that MCs in the whisker FSC contribute to cortical encoding of both whisker amplitude and velocity, mainly by tuning wS1 response magnitude, and by patterning the evoked spiking activity. As wS1 neurons retained the ability to differentiate stimulus features based on the timing of their first post-stimulus spike, MCs are thus suggested to play secondary roles over other LTMRs in tuning cortical response latency. While the present study allowed to replicate a recent finding on the role played by MCs in tuning S1 sensitivity in response to cutaneous touch (Emanuel et al., 2021), its results and interpretation were based on a relatively small sample size. Further investigations are thus required to confirm the proposed roles played by MCs in cortical encoding of whisker amplitude and velocity.

## Funding information

This project was supported by the Deutsche Forschungsgemeinschaft (DFG, German Research Foundation, www.dfg.de; SFB874/A9, project number: 122679504 to P.K.). The funding organization had no role in study design, data collection and analysis, decision to publish, or preparation of the manuscript.

## Conflict of interest statement

Neither of the authors reports a conflict of interest.

## Data Availability

The data supporting this study can be made available upon reasonable request to the corresponding author.

## Acknowledgments

The authors thank Prof. Ellen Lumpkin (Department of Physiology & Cellular Biophysics, Columbia University, New York, NY 10032) for the gift of the transgenic mouse lines and Ute Neubacher (Manahan-Vaughan lab, Department of Neurophysiology, Medical Faculty, Ruhr University Bochum) for helpful assistance in histology and imaging.

### *Author contributions statement*

C.E.L. and P.K. designed the research. C.E.L. performed the experiments, analyzed the data, and wrote the paper.

## Appendix A. Supporting information

Supplementary data associated with this article can be found in the online version at doi:10.1016/j.ibneur.2022.09.008.

## References

Abraira, V.E., Ginty, D.D., 2013. The sensory neurons of touch. Neuron 79, 618–639. https://doi.org/10.1016/j.neuron.2013.07.051.

Adibi, M., 2019. Whisker-mediated touch system in rodents: from neuron to behavior. Front. Syst. Neurosci. 13, 40. https://doi.org/10.3389/fnsys.2019.00040.

Adibi, M., Lampl, I., 2021. Sensory adaptation in the whisker-mediated tactile system: physiology, theory, and function. Front. Neurosci. 15, 770011 https://doi.org/10.3389/fnins.2021.770011.

Ahissar, E., Sosnik, R., Bagdasarian, K., Haidarliu, S., 2001. Temporal frequency of whisker movement. II. Laminar organization of cortical representations. J. Neurophysiol. 86, 354–367. https://doi.org/10.1152/jn.2001.86.1.354.

Ahissar, E., Sosnik, R., Haidarliu, S., 2000. Transformation from temporal to rate coding in a somatosensory thalamocortical pathway. Nature 406, 302–306. https://doi.org/10.1038/35018568.

Arabzadeh, E., Zorzin, E., Diamond, M.E., 2005. Neuronal encoding of texture in the whisker sensory pathway. PLoS Biol. 3, e17 https://doi.org/10.1371/journal.pbio.0030017.

Bale, M.R., Campagner, D., Erskine, A., Petersen, R.S., 2015. Microsecond-scale timing precision in rodent trigeminal primary afferents. J. Neurosci. 35, 5935–5940. https://doi.org/10.1523/JNEUROSCI.3876-14.2015.

Bale, M.R., Petersen, R.S., 2009. Transformation in the neural code for whisker deflection direction along the lemniscal pathway. J. Neurophysiol. 102, 2771–2780. https://doi.org/10.1152/jn.00636.2009.

Bosman, L.W.J., Houweling, A.R., Owens, C.B., Tanke, N., Shevchouk, O.T., Rahmati, N., Teunissen, W.H.T., Ju, C., Gong, W., Koekkoek, S.K.E., De Zeeuw, C.I., 2011. Anatomical pathways involved in generating and sensing rhythmic whisker movements. Front. Integr. Neurosci. 5. https://doi.org/10.3389/fnint.2011.00053.

Chang, W., Kanda, H., Ikeda, R., Ling, J., DeBerry, J.J., Gu, J.G., 2016. Merkel disc is a serotonergic synapse in the epidermis for transmitting tactile signals in mammals. Proc. Natl. Acad. Sci. U.S.A. 113. https://doi.org/10.1073/pnas.1610176113.

Diamond, M.E., von Heimendahl, M., Arabzadeh, E., 2008. Whisker-mediated texture discrimination. PLoS Biol. 6, e220 https://doi.org/10.1371/journal.pbio.0060220.

Ebara, S., Kumamoto, K., Matsuura, T., Mazurkiewicz, J.E., Rice, F.L., 2002. Similarities and differences in the innervation of mystacial vibrissal follicle-sinus complexes in the rat and cat: A confocal microscopic study. J. Comp. Neurol. 449, 103–119. https://doi.org/10.1002/cne.10277.

Emanuel, A.J., Lehnert, B.P., Panzeri, S., Harvey, C.D., Ginty, D.D., 2021. Cortical responses to touch reflect subcortical integration of LTMR signals. Nature 600, 680–685. https://doi.org/10.1038/s41586-021-04094-x.

Fundin, B.T., Rice, F.L., Pfaller, K., Arvidsson, J., 1994. The innervation of the mystacial pad in the adult rat studied by anterograde transport of HRP conjugates. Exp. Brain Res. 99. https://doi.org/10.1007/BF00239590.

Furuta, T., Bush, N.E., Yang, A.E.-T., Ebara, S., Miyazaki, N., Murata, K., Hirai, D., Shibata, K., Hartmann, M.J.Z., 2020. The cellular and mechanical basis for response characteristics of identified primary afferents in the rat vibrissal system. e5 Curr. Biol. 30, 815–826. https://doi.org/10.1016/j.cub.2019.12.068.

Ganmor, E., Katz, Y., Lampl, I., 2010. Intensity-dependent adaptation of cortical and thalamic neurons is controlled by brainstem circuits of the sensory pathway. Neuron 66, 273–286. https://doi.org/10.1016/j.neuron.2010.03.032.

Gottschaldt, K., Vahle-Hinz, C., 1981. Merkel cell receptors: structure and transducer function. Science 214 (4517), 183–186. https://doi.org/10.1126/science.7280690.

Gottschaldt, K.-M., Iggo, A., Young, D.W., 1973. Functional characteristics of mechanoreceptors in sinus hair follicles of the cat. J. Physiol. 235, 287–315. https://doi.org/10.1113/jphysiol.1973.sp010388.

Halata, Z., Grim, M., Bauman, K.I., 2003. Friedrich sigmund merkel and his ?Merkel cell?, Morphology, development, and physiology: review and new results. Anat. Rec. 271A, 225–239. https://doi.org/10.1002/ar.a.10029.

Hayasaki, H., Sohma, Y., Kanbara, K., Maemura, K., Kubota, T., Watanabe, M., 2006. A local GABAergic system within rat trigeminal ganglion cells. Eur. J. Neurosci. 23, 745–757. https://doi.org/10.1111/j.1460-9568.2006.04602.x.

Higashikawa, A., Kimura, M., Shimada, M., Ohyama, S., Ofusa, W., Tazaki, M., Shibukawa, Y., 2019. Merkel cells release glutamate following mechanical deflection: implication of glutamate in the merkel cell-neurite complex. Front. Cell. Neurosci. 13, 255. https://doi.org/10.3389/fncel.2019.00255.

Hoffman, B.U., Baba, Y., Griffith, T.N., Mosharov, E.V., Woo, S.-H., Roybal, D.D., Karsenty, G., Patapoutian, A., Sulzer, D., Lumpkin, E.A., 2018. Merkel cells activate sensory neural pathways through adrenergic synapses. Neuron 100 (1401–1413), e6. https://doi.org/10.1016/j.neuron.2018.10.034.

Iggo, A., Muir, A.R., 1969. The structure and function of a slowly adapting touch corpuscle in hairy skin. J. Physiol. 200, 763–796. https://doi.org/10.1113/jphysiol.1969.sp008721.

Ikeda, I., Yamashita, Y., Ono, T., Ogawa, H., 1994. Selective phototoxic destruction of rat Merkel cells abolishes responses of slowly adapting type I mechanoreceptor units. J. Physiol. 479, 247–256. https://doi.org/10.1113/jphysiol.1994.sp020292.

Ikeda, R., Cha, M., Ling, J., Jia, Z., Coyle, D., Gu, J.G., 2014. Merkel cells transduce and encode tactile stimuli to drive Aβ-afferent impulses. Cell 157, 664–675. https://doi.org/10.1016/j.cell.2014.02.026.

Ito, M., 1985. Processing of vibrissa sensory information within the rat neocortex. J. Neurophysiol. 54, 479–490. https://doi.org/10.1152/jn.1985.54.3.479.

Ito, M., Kato, M., 2002. Analysis of variance study of the rat cortical layer 4 barrel and layer 5b neurones. J. Physiol. 539, 511–522. https://doi.org/10.1113/jphysiol.2001.013004.

Jones, L.M., Depireux, D.A., Simons, D.J., Keller, A., 2004. Robust temporal coding in the trigeminal system. Science 304, 1986–1989. https://doi.org/10.1126/science.1097779.

Krieger, P., Groh, A., 2015. Sensorimotor Integration in the Whisker System, first ed. Springer-Verlag. https://doi.org/10.1007/978-1-4939-2975-7.

Kwegyir-Afful, E.E., Marella, S., Simons, D.J., 2008. Response properties of mouse trigeminal ganglion neurons. Somatosens. Mot. Res. 25, 209–221. https://doi.org/10.1080/08990220802467612.

Land, P.W., Simons, D.J., 1985. Cytochrome oxidase staining in the rat smI barrel cortex. J. Comp. Neurol. 238, 225–235. https://doi.org/10.1002/cne.902380209.

Lauer, S.M., Schneeweiß, U., Brecht, M., Ray, S., 2018. Visualization of cortical modules in flattened mammalian cortices. JoVE 56992. https://doi.org/10.3791/56992.

Lottem, E., Gugig, E., Azouz, R., 2015. Parallel coding schemes of whisker velocity in the rat's somatosensory system. J. Neurophysiol. 113, 1784–1799. https://doi.org/10.1152/jn.00485.2014.

Maksimovic, S., Nakatani, M., Baba, Y., Nelson, A.M., Marshall, K.L., Wellnitz, S.A., Firozi, P., Woo, S.-H., Ranade, S., Patapoutian, A., Lumpkin, E.A., 2014. Epidermal Merkel cells are mechanosensory cells that tune mammalian touch receptors. Nature 509, 617–621. https://doi.org/10.1038/nature13250.

Maricich, S.M., Morrison, K.M., Mathes, E.L., Brewer, B.M., 2012. Rodents rely on merkel cells for texture discrimination tasks. J. Neurosci. 32, 3296–3300. https://doi.org/10.1523/JNEUROSCI.5307-11.2012.

Maricich, S.M., Wellnitz, S.A., Nelson, A.M., Lesniak, D.R., Gerling, G.J., Lumpkin, E.A., Zoghbi, H.Y., 2009. Merkel cells are essential for light-touch responses. Science 324, 1580–1582. https://doi.org/10.1126/science.1172890.

Morrison, K.M., Miesegaes, G.R., Lumpkin, E.A., Maricich, S.M., 2009. Mammalian Merkel cells are descended from the epidermal lineage. Dev. Biol. 336, 76–83. https://doi.org/10.1016/j.ydbio.2009.09.032.

Nakatani, M., Maksimovic, S., Baba, Y., Lumpkin, E.A., 2015. Mechanotransduction in epidermal Merkel cells. Pflug. Arch. - Eur. J. Physiol. 467, 101–108. https://doi.org/10.1007/s00424-014-1569-0.

Pammer, L., O'Connor, D.H., Hires, S.A., Clack, N.G., Huber, D., Myers, E.W., Svoboda, K., 2013. The mechanical variables underlying object localization along the axis of the whisker. J. Neurosci. 33, 6726–6741. https://doi.org/10.1523/JNEUROSCI.4316-12.2013.

Panzeri, S., Petersen, R.S., Schultz, S.R., Lebedev, M., Diamond, M.E., 2001. The role of spike timing in the coding of stimulus location in rat somatosensory cortex. Neuron 29, 769–777. https://doi.org/10.1016/S0896-6273(01)00251-3.

Petersen, C.C.H., 2007. The functional organization of the barrel cortex. Neuron 56, 339–355. https://doi.org/10.1016/j.neuron.2007.09.017.

Petersen, R.S., Panzeri, S., Diamond, M.E., 2001. Population coding of stimulus location in rat somatosensory cortex. Neuron 32, 503–514. https://doi.org/10.1016/S0896-6273(01)00481-0.

Pinto, D.J., Brumberg, J.C., Simons, D.J., 2000. Circuit dynamics and coding strategies in rodent somatosensory cortex. J. Neurophysiol. 83, 1158–1166. https://doi.org/10.1152/jn.2000.83.3.1158.

Pohlert, T., 2020. PMCMRplus: calculate pairwise multiple comparisons of mean rank sums extended. R. Package Version 1. 4. 4. ⟨https://CRAN.R-project.org/package=PMCMRplus⟩.

R Core Team, 2021 R: A language and environment for statistical computing. Vienna, Austria: R Foundation for Statistical Computing ⟨https://www.R-project.org/⟩.

Rice, F.L., Fundin, B.T., Arvidsson, J., Aldskogius, H., Johansson, O., 1997. Comprehensive immunofluorescence and lectin binding analysis of vibrissal follicle sinus complex innervation in the mystacial pad of the rat. J. Comp. Neurol. 385, 149–184. https://doi.org/10.1002/(SICI)1096-9861(19970825)385:2<149::AID-CNE1>3.0.CO;2-1.

Rice, F.L., Mance, A., Munger, B.L., 1986. A comparative light microscopic analysis of the sensory innervation of the mystacial pad. I. Innervation of vibrissal follicle-sinus

complexes. J. Comp. Neurol. 252, 154–174. https://doi.org/10.1002/cne.902520203.
Sakurai, K., Akiyama, M., Cai, B., Scott, A., Han, B.-X., Takatoh, J., Sigrist, M., Arber, S., Wang, F., 2013. The organization of submodality-specific touch afferent inputs in the vibrissa column. Cell Rep. 5, 87–98. https://doi.org/10.1016/j.celrep.2013.08.051.
Severson, K.S., Xu, D., Van de Loo, M., Bai, L., Ginty, D.D., O'Connor, D.H., 2017. Active touch and self-motion encoding by merkel cell-associated afferents. e9 Neuron 94, 666–676. https://doi.org/10.1016/j.neuron.2017.03.045.
Severson, K.S., Xu, D., Yang, H., O'Connor, D.H., 2019. Coding of whisker motion across the mouse face. eLife 23, e41535. https://doi.org/10.7554/eLife.41535.
Shoykhet, Donald Doherty, Daniel, J.M., 2000. Coding of deflection velocity and amplitude by whisker primary afferent neurons: implications for higher level processing. Somatosens. Mot. Res. 17, 171–180. https://doi.org/10.1080/08990220050020580.
Stüttgen, M.C., Kullmann, S., Schwarz, C., 2008. Responses of rat trigeminal ganglion neurons to longitudinal whisker deflection. J. Neurophysiol. 100, 6. https://doi.org/10.1152/jn.90511.2008.
Szwed, M., Bagdasarian, K., Ahissar, E., 2003. Encoding of vibrissal active touch. Neuron 40, 621–630. https://doi.org/10.1016/S0896-6273(03)00671-8.
Tonomura, S., Ebara, S., Bagdasarian, K., Uta, D., Ahissar, E., Meir, I., Lampl, I., Kuroda, D., Furuta, T., Furue, H., Kumamoto, K., 2015. Structure-function correlations of rat trigeminal primary neurons: emphasis on club-like endings, a vibrissal mechanoreceptor. Proc. Jpn. Acad. Ser. B: Phys. Biol. Sci. 91, 560–576. https://doi.org/10.2183/pjab.91.560.
Van Keymeulen, A., Mascre, G., Youseff, K.K., Harel, I., Michaux, C., De Geest, N., Szpalski, C., Achouri, Y., Bloch, W., Hassan, B.A., Blanpain, C., 2009. Epidermal progenitors give rise to Merkel cells during embryonic development and adult homeostasis. J. Cell Biol. 187, 91–100. https://doi.org/10.1083/jcb.200907080.
Welker, C., Woolsey, T.A., 1974. Structure of layer IV in the somatosensory neocortex of the rat: description and comparison with the mouse. J. Comp. Neurol. 158, 437–453. https://doi.org/10.1002/cne.901580405.
Whiteley, S.J., Knutsen, P.M., Matthews, D.W., Kleinfeld, D., 2015. Deflection of a vibrissa leads to a gradient of strain across mechanoreceptors in a mystacial follicle. J. Neurophysiol. 114, 138–145. https://doi.org/10.1152/jn.00179.2015.
Wickham, H., 2016. ggplot2: Elegant Graphics for Data Analysis. Springer-Verlag, New York. ISBN 978-3-319-24277-4. ⟨https://ggplot2.tidyverse.org⟩.
Wilent, W.B., Contreras, D., 2004. Synaptic responses to whisker deflections in rat barrel cortex as a function of cortical layer and stimulus intensity. J. Neurosci. 24, 3985–3998. https://doi.org/10.1523/JNEUROSCI.5782-03.2004.
Woo, S.-H., Lumpkin, E.A., Patapoutian, A., 2015. Merkel cells and neurons keep in touch. Trends Cell Biol. 25, 74–81. https://doi.org/10.1016/j.tcb.2014.10.003.
Woo, S.-H., Ranade, S., Weyer, A.D., Dubin, A.E., Baba, Y., Qiu, Z., Petrus, M., Miyamoto, T., Reddy, K., Lumpkin, E.A., Stucky, C.L., Patapoutian, A., 2014. Piezo2 is required for Merkel-cell mechanotransduction. Nature 509, 622–626. https://doi.org/10.1038/nature13251.
Woo, S.-H., Stumpfova, M., Jensen, U.B., Lumpkin, E.A., Owens, D.M., 2010. Identification of epidermal progenitors for the Merkel cell lineage, 622–622 Development 139. https://doi.org/10.1242/dev.077990.
Yamamoto, M., Wada, N., Kitabatake, Y., Watanabe, D., Anzai, M., Yokoyama, M., Teranishi, Y., Nakanishi, S., 2003. Reversible suppression of glutamatergic neurotransmission of cerebellar granule cells *In Vivo* by genetically manipulated expression of tetanus neurotoxin light chain. J. Neurosci. 23, 6759–6767. https://doi.org/10.1523/JNEUROSCI.23-17-06759.2003.
Zehendner, C.M., Luhmann, H.J., Yang, J.-W., 2013. A simple and novel method to monitor breathing and heart rate in awake and urethane-anesthetized newborn rodents. PLoS One 8, e62628. https://doi.org/10.1371/journal.pone.0062628.